Nitrogen Photofixation | Hot Paper

DOI: 10.1002/ange.201404748

Plasmon-Induced Ammonia Synthesis through Nitrogen Photofixation with Visible Light Irradiation**

*Tomoya Oshikiri, Kosei Ueno, and Hiroaki Misawa**

Abstract: *We have successfully developed a plasmon-induced technique for ammonia synthesis that responds to visible light through a strontium titanate ($SrTiO_3$) photoelectrode loaded with gold (Au) nanoparticles. The photoelectrochemical reaction cell was divided into two chambers to separate the oxidized (anodic side) and reduced (cathodic side) products. To promote NH_3 formation, a chemical bias was applied by regulating the pH value of these compartments, and ethanol was added to the anodic chamber as a sacrificial donor. The quantity of NH_3 formed at the ruthenium surface, which was used as a co-catalyst for $SrTiO_3$, increases linearly as a function of time under irradiation with visible light at wavelengths longer than 550 nm. The NH_3 formation action spectrum approximately corresponds to the plasmon resonance spectrum. We deduced that plasmon-induced charge separation at the Au/$SrTiO_3$ interface promotes oxidation at the anodic chamber and subsequent nitrogen reduction on the cathodic side.*

To solve global energy and environmental problems, an artificial photosynthesis system that enables solar energy conversion into chemical materials, such as hydrogen, is indispensable. However, hydrogen is not suitable for storage and transportation because it has a large volume and easily penetrates into its container. Ammonia has garnered attention as a potential hydrogen carrier and a fuel for vehicles.[1] Furthermore, it is easily condensed to a liquid, and has a high hydrogen content (17.6 wt%).

Ammonia synthesis is performed using the Haber–Bosch process with a catalyst at 400–600 °C and 20–40 MPa,[2] and it consumes more than 1% of the world's power production.[3] Developing nitrogen fixation under ambient conditions is one of the most crucial subjects in chemistry. For example, numerous researchers have attempted to synthesize ammonia by a thermal reaction with an improved catalyst,[4] a photocatalytic reaction,[5] or an electrochemical reaction through applying an external bias between the electrodes.[6]

Fujishima and Honda discovered the photo-electrochemical splitting of water using a titanium dioxide (TiO_2) photoelectrode under irradiation by ultraviolet light.[7] They showed that TiO_2 is an excellent photocatalyst for redox reactions. Guth and Schrauzer reported for the first time that the electron-hole pairs generated by the absorption of light in a rutile-containing TiO_2 powder reduce molecular nitrogen to ammonia. In that case, excitation by ultraviolet light was required.[8]

However, only approximately 5% of the solar irradiance observed on earth's surface is ultraviolet radiation (<400 nm), whereas visible light (400–800 nm) comprises 50% and infrared light (>800 nm) comprises the remaining 45%. Therefore, extending light-energy conversion to longer wavelengths, especially in the visible and near-infrared wavelength regions, is an important goal.[9] Recently, Kisch and coworkers reported nitrogen photofixation using a nanostructured iron titanate film initiated by visible light ($\lambda>$ 455 nm).[10] However, in that case, the ammonia formed was quickly oxidized to nitrate. One of the drawbacks of using a semiconductor as a photocatalytic redox system is that energy is necessary to separate the reduction and oxidation products because they are produced in the same reaction chamber.

Noble metal nanoparticles that show localized surface plasmon resonance (LSPR) when deposited on a semiconductor photoelectrode may potentially promote photo-electrochemical water splitting because of the light-harvesting effect in the visible wavelength region. Interestingly, LSPR significantly separates photogenerated electrons and holes at a semiconductor/metal interface following electron transfer from an excited metallic nanoparticle to the conduction band of a n-type semiconductor or hot-electron transfer, which promote a photocurrent enhancement and water oxidation.[11] Previously we successfully demonstrated plasmon-enhanced photocurrent generation and water oxidation through irradiation with visible and near-infrared light by using a TiO_2 single-crystal photoelectrode loaded with gold nanoparticles (Au NPs).[12]

Here, we report a plasmon-induced ammonia synthesis device that responds to visible light through a semiconductor photoelectrode loaded with Au NPs. In this study, 0.05 wt% niobium (Nb) doped strontium titanate (Nb-$SrTiO_3$) with a band gap of 3.2 eV, which is comparable to TiO_2 anatase, was employed as a semiconductor photoelectrode for efficient NH_3 formation. The NH_3 synthesis device contains two compartments to separate the reduced and oxidation prod-

[*] Dr. T. Oshikiri, Prof. K. Ueno, Prof. H. Misawa
Research Institute for Electronic Science
Hokkaido University N21, W10, CRIS Bldg.
Kita-ku, Sapporo 001-0021 (Japan)
E-mail: misawa@es.hokudai.ac.jp
Homepage: http://misawa.es.hokudai.ac.jp/index_en.html

[**] This study was supported by funding from the Ministry of Education, Culture, Sports, Science, and Technology of Japan: KAKENHI Grant-in-Aid for Scientific Research (s) (no. 23225006), Grant-in-Aid for Research Activity Start-up (no. 25888002) and the Innovative Areas "Artificial Photosynthesis (AnApple)" (no. 25107501) grant from the Japan Society for the Promotion of Science (JSPS), the Nanotechnology Platform (Hokkaido University), and the Low-Carbon Research Network of Japan.

Supporting information for this article is available on the WWW under http://dx.doi.org/10.1002/anie.201404748.

ucts. To promote NH_3 formation, a chemical bias was applied by regulating the pH value of these compartments rather than using an external electrochemical apparatus. The anodic chamber was filled with an aqueous solution of potassium hydroxide (KOH). Simultaneously, an aqueous solution of hydrogen chloride (HCl) was injected into the cathodic chamber with nitrogen gas. HCl also serves as a proton source for ammonia synthesis. In addition, ethanol was added to the anodic compartment as a sacrificial donor. The principle of this device relies on a plasmon-induced charge separation at the Au NPs/Nb-$SrTiO_3$ interface that promotes efficient water and ethanol oxidation and subsequent nitrogen reduction at the ruthenium surface, which was used as a co-catalyst for Nb-$SrTiO_3$.

Scanning electron microscope images of Au NPs fabricated by using an annealing method, and Ru deposited using the electron beam evaporation method, on the 0.05 wt% Nb-$SrTiO_3$ single-crystal substrate are shown in Figure 1a,b, respectively. The average Au NP size was 48 nm, and the standard deviation for the size was estimated to be 17 nm. In addition, Ru was deposited as a nanoparticulate solid. Figure 1c indicates an extinction spectrum of the Au NPs on the Nb-$SrTiO_3$ substrate. The data clearly show that the LSPR band reached a maximum at 630 nm. A schematic illustration of the NH_3 synthesis system using a Nb-$SrTiO_3$ substrate loaded with Au NPs is shown in Figure 1d. In the front chamber (anodic side), water and ethanol oxidation reactions are expected following the plasmon-induced charge separation. NH_3 formation is expected in the rear chamber (cathodic side) as a result of nitrogen reduction by photogenerated electrons injected into the Nb-$SrTiO_3$ conduction band at the Ru surface, which is used as a co-catalyst for $SrTiO_3$. All photo-electrochemical experiments were conducted at room temperature, and an effect of local heating is negligible because the xenon lamp is too weak to induce the effective local heating through LSPR.[13]

Figure 2a depicts the dependence of NH_3 formation in the cathodic chambers on the irradiation time. The Au NPs were irradiated at 550 nm to 800 nm with spectrally filtered xenon light to excite the LSPR. Under the irradiation conditions, NH_3 formation increased linearly with the irradiation time, and the reaction rate for NH_3 formation was 0.231 nmol h^{-1}. However, NH_3 formation from the Nb-$SrTiO_3$ substrate without Au NPs under the same irradiation conditions showed no time dependency. Of course, no time dependency for NH_3 formation was observed without irradiation over a long time period (24 h), even when using a Nb-$SrTiO_3$ substrate loaded with Au NPs. In addition, when the Nb-$SrTiO_3$ substrate was irradiated with light including the ultraviolet region under an argon atmosphere instead of N_2, we observed little NH_3 production (see Figure S3 in the Supporting Information).

The histogram in Figure 2b shows the action spectrum for the apparent quantum efficiency of the NH_3 formation η_{app,NH_3}. In the 550–800 nm region, the η_{app,NH_3} value approximately correlates with the LSPR band, which is indicated by the solid line in Figure 2b, whereas the η_{app,NH_3} value in the 410 to 550 nm wavelength region was higher than the spectrum for Au NPs on Nb-$SrTiO_3$. These data indicate that NH_3 was formed not only by the LSPR excitation but also by the direct excitation of the interband transition from d bands to the sp conduction band of gold in the 410–550 nm wavelength region. Thus, the efficiency of NH_3 formation in the shorter wavelength region at 410–550 nm is higher than in the longer

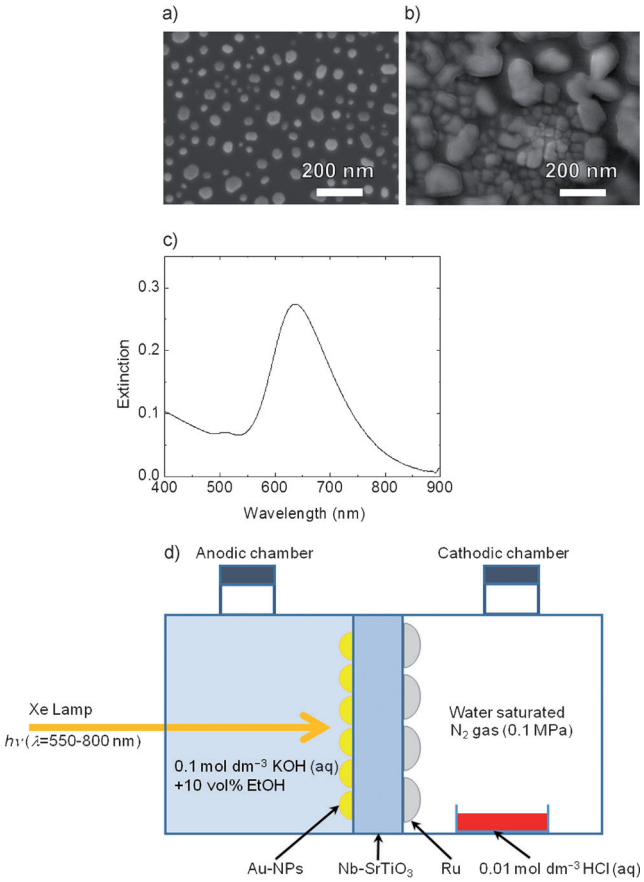

Figure 1. a) Scanning electron microscope image of Au NPs on Nb-$SrTiO_3$, prepared using the annealing method. b) Scanning electron microscope image of Ru on Nb-$SrTiO_3$, prepared using the electron beam evaporation method. c) Extinction spectrum of the Au NPs on Nb-$SrTiO_3$. d) A schematic illustration of the NH_3 synthesis device using a Nb-$SrTiO_3$ photoelectrode loaded with Au NPs.

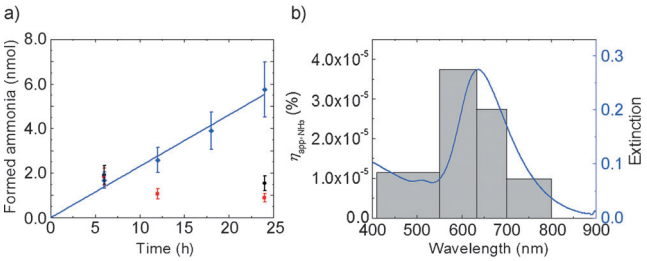

Figure 2. a) Dependence of NH_3 formation on the cathodic side of the chamber on the irradiation time. Nb-$SrTiO_3$ with irradiation (red square); Nb-$SrTiO_3$ loaded with Au NPs and Ru without irradiation (black circle); and Nb-$SrTiO_3$ loaded with Au NPs and Ru with irradiation (blue diamond). The irradiation condition included xenon light spectrally filtered to 550–800 nm. b) Histogram of the action spectrum of the apparent quantum efficiency of NH_3 formation for several wavelength regions. The solid line indicates the LSPR band, which is also shown in Figure 1c.

wavelength region at 700–800 nm. It is worth noting that NH_3 formation was highly related to the LSPR excitation, as the apparent quantum efficiency of NH_3 formation was highly dependent on the LSPR band. In addition, when the same procedure was demonstrated for smaller Au NPs on Nb-$SrTiO_3$, which display a LSPR band in the shorter wavelengths, the action spectrum of η_{app,NH_3} also showed good agreement with the LSPR band (see Figure S4 in the Supporting Information).

In this system, four primary types of reactions proceed in accordance with Equations (1)–(4), where $U°$, e^-, and h^+ indicate the standard redox potential, electron, and hole, respectively. The oxidized and reduced products were detected and quantified by colorimetric quantification and gas chromatography methods. On the cathodic electrode, Equations (1) and (2) occur:

$$N_2 + 6\,H^+ + 6\,e^- \rightarrow 2NH_3 \qquad U°(N_2/NH_3): \ -0.092\ \text{V versus RHE} \tag{1}$$

$$2\,H^+ + 2\,e^- \rightarrow H_2 \qquad U°(H^+/H_2): \ 0\ \text{V versus RHE} \tag{2}$$

On the anodic electrode, Equations (3) and (4) occur:

$$C_2H_5OH + 2\,h^+ \rightarrow CH_3CHO + 2\,H^+ \qquad U°(CH_3CHO/EtOH): \ 0.216\ \text{V versus RHE} \tag{3}$$

$$4\,OH^- + 4\,h^+ \rightarrow 2\,H_2O + O_2 \qquad U°(O_2/H_2O): \ 1.23\ \text{V versus RHE} \tag{4}$$

The following reaction rates were obtained: 3.76 nmol h^{-1} for H_2 evolution, 1.20 nmol h^{-1} for O_2 evolution, and 1.82 nmol h^{-1} for CH_3CHO formation. O_2 evolution was clearly observed even though $U°(O_2/H_2O)$ is much more positive than $U°(CH_3CHO/EtOH)$, as described by Equations (3) and (4). Efficient OH^- oxidation requires highly concentrated electron holes at a local site, because multiple electron-transfer processes are required with four OH^- ions. The LSPR may generate multiple holes trapped at the $SrTiO_3$ surface states near the hot site, which might be stored at a local $SrTiO_3$ site. The multiple stored holes confined at a local site on the $SrTiO_3$ may accelerate the oxidation of hydroxy ions and subsequent oxygen evolution. In the cathodic chamber, the H_2 evolution was observed in addition to NH_3 formation. It is well known that Ru is a good catalyst not only for N_2 reduction but also for H_2 evolution,[14] because H_2 strongly adsorbs onto a ruthenium surface.[15] Furthermore, the relatively slow rate of NH_3 formation may also represent a larger activation energy required to cleave the triple bond of the nitrogen molecule compared with the energy required to produce a hydrogen molecule from protons.

These redox reactions proceeded with electrons and holes generated by LSPR excitation. Figure 3a indicates the number of electrons and holes per second that reacted in the reduction and oxidization reactions on the cathodic and anodic sides, respectively. The numbers of electrons on the cathodic side and holes on the anodic side were highly

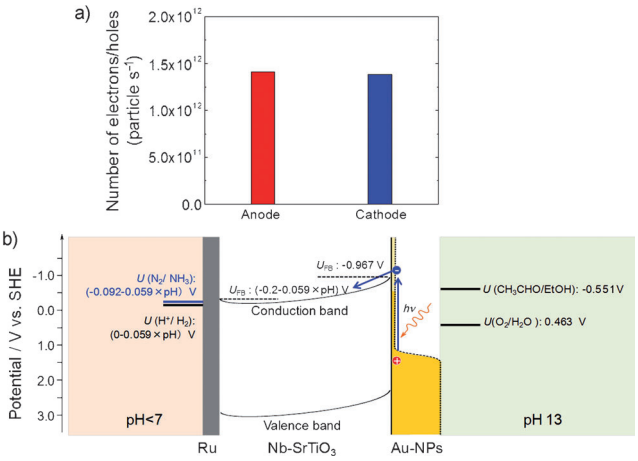

Figure 3. a) The number of electrons and holes that react per second derived from the reduction and oxidization on the cathodic and anodic sides, respectively. b) An energy diagram of the plasmon-induced ammonia photosynthesis system using a $SrTiO_3$ substrate loaded with Au NPs. The flat band potential for $SrTiO_3$ on the cathodic side was estimated to be −0.2–0.059 × pH V versus SHE because the $SrTiO_3$ conduction band potential is −0.2 V versus SHE at pH 0. The pH value for the cathodic surface of $SrTiO_3$ was less than 7 because a volatile aqueous solution of HCl (0.01 mol dm^{-3}) was injected into the cathodic chamber.

consistent. Therefore, we have confirmed a stoichiometric reaction within the full redox system.

Figure 3b illustrates an energy diagram for the plasmon-induced system for the photosynthesis of NH_3 using a $SrTiO_3$ photoelectrode loaded with Au NPs. It was hypothesized that an excited electron is transferred to the $SrTiO_3$ conduction band immediately following the Au NP inter- or intraband transition induced by the plasmonically enhanced optical near-field or by hot electron transfer. These events yielded a hole trapped in the $SrTiO_3$ surface near the Au/$SrTiO_3$/water interface; subsequently, the trapped holes can efficiently induce oxidation of hydroxy ions and ethanol through multielectron transfer. By contrast, the photogenerated electrons injected into the conduction band of $SrTiO_3$ induced nitrogen and proton reduction at the Ru surface, which was deposited on the rear of the $SrTiO_3$. In the anodic chamber, the potentials shifted negatively because the pH value was fixed at 13 by the aqueous KOH solution that filled the chamber. Simultaneously, in the cathodic chamber, potentials shifted positively because the pH value was fixed to acidic through adsorbed HCl derived from an injected aqueous solution of HCl (0.01 mol dm^{-3}). The chemical bias accelerates the reaction. Thus, plasmon-induced ammonia photosynthesis through nitrogen photofixation was clearly demonstrated.

In summary, we have successfully developed a stable and simple plasmon-induced ammonia synthesis system without an external electrochemical apparatus by using two sides of the same $SrTiO_3$ single-crystal substrate. The NH_3 formation action spectrum was highly consistent with the LSPR band. To the best of our knowledge, this system is the first example of NH_3 synthesis through N_2 photofixation under irradiation with visible light that includes only wavelength bands longer than 550 nm. A kinetic study revealed that the cathodic

reaction and anodic reaction were stoichiometrically balanced, and the electrons on the cathode were consumed not only for NH_3 formation, but also for H_2 production. Therefore, it may be possible to construct an efficient artificial ammonia photosynthesis system that responds to visible and near-infrared light after the selective and efficient co-catalysts are combined for N_2 photofixation.

Experimental Section

Preparation of Au NPs on a $SrTiO_3$ substrate: Single-crystal $SrTiO_3$ (0.05 wt% niobium-doped, $10\times10\times0.5\ mm^3$, Furuuchi Chemical) with a (110) surface was used as a semiconductor substrate for N_2 photofixation. The $SrTiO_3$ substrate as purchased was rinsed with acetone, methanol, and deionized water in an ultrasonic bath for 5 min followed by drying under a pure nitrogen flow. Next, the substrate was exposed to O_3 for 5 min by an excimer lamp (PC-01-H, N-Cobo) irradiation under an O_2 atmosphere. A 3 nm thin gold film was deposited on the front side of the $SrTiO_3$ through helicon sputtering (MPS-4000, ULVAC) with a deposition rate of $0.1\ nm\,s^{-1}$ and annealed at 800 °C for 1 h in a nitrogen atmosphere to form Au NPs on the $SrTiO_3$ surface.[11] On the other hand, a thin 3 nm Ru layer was deposited on the opposite side of the $SrTiO_3$ substrate through electron-beam deposition (ED-1500R, SUNVAC) at a deposition rate of $0.05\ nm\,s^{-1}$. The Au NPs and Ru on the $SrTiO_3$ were observed using field-emission scanning electron microscopy (FE-SEM, JSM-6700FT, JEOL); the maximum resolution attainable at an electron acceleration voltage of 15 kV was 1 nm.

Construction of the NH_3 synthesis device: The N_2 photofixation device comprised sealed reaction cells with two compartments separated by the $SrTiO_3$ substrate. The surface with Au NPs was on the front of the photoelectrode, which was irradiated with visible light for the oxidation reaction, while the thin Ru film was used for NH_3 formation on the rear. To adjust the chemical bias between the front and rear chambers, the pH value was regulated using aqueous solutions of KOH and HCl. The anodic chamber, with a volume of 500 μL, was filled with an aqueous solution of KOH and ethanol (9:1 v/v) at pH 13; however, the cathodic chamber, with a volume of 200 μL, was filled with water saturated nitrogen gas. Next, 15 μL of an aqueous solution of HCl was injected into the cathodic chamber.

Photoelectrochemical reaction: The gold nanostructured $SrTiO_3$ substrate was irradiated over an area with a diameter of 6 mm by a xenon lamp using an arbitrary light intensity and wavelength.

The η_{app} value of the NH_3 formation system, in which three photons are theoretically required to produce one NH_3 molecule, was determined using Equation (5),

$$\eta_{app,NH3}(\%) = \frac{[\text{Reaction rate of } NH_3 \text{ formation } (\text{mol}\,s^{-1})]\times 3}{[\text{Incident photon flux } (\text{mol}\,s^{-1})]}\times 100 \quad (5)$$

The incident photon flux was measured using a spectroradiometer (MSR-7000N, optoresearch) at each wavelength.

Quantitative determination of NH_3: The quantity of NH_3 formation was determined by a colorimetric method using sodium salicylate, pyrazole, sodium hypochlorite, and sodium hydroxide.[16] See the Supporting Information for full details).

Quantitative determination of aldehyde: The quantity of acetaldehyde formed was determined by a colorimetric method using 3-methyl-2-benzothiazolinone hydrazone hydrochloride monohydrate, iron(III) chloride, and hydrochloric acid.[17] See the Supporting Information for full details.

Quantitative determination of H_2 and O_2 evolution: The quantity of evolved O_2 and H_2 was determined using gas chromatography/mass spectroscopy (GC-MS 2010-plus, Shimadzu) and gas chromatography/thermal conductivity detector (GC-TCD 2014, Shimadzu) respectively. See the Supporting Information for full details.

Received: April 28, 2014
Published online: July 17, 2014

Keywords: ammonia · localized surface plasmon · nanostructures · nitrogen fixation · photochemistry

[1] a) L. J. Green, Jr., *Int. J. Hydrogen Energy* **1982**, *7*, 355–359; b) A. Klerke, C. H. Christensen, J. K. Nørskov, T. Vegge, *J. Mater. Chem.* **2008**, *18*, 2304; c) R. Lan, J. T. S. Irvine, S. Tao, *Int. J. Hydrogen Energy* **2012**, *37*, 1482–1494.
[2] a) *Fundamentals and Practice* (Ed.: J. R. Jennings), Plemium, New York, **1991**; b) K. Aika, L. J. Chiristiansen, I. Dybkjacr, J. B. Hansen, H. Nielsen, A. Nielsen, P. Stoltze, K. Tamaru, *Catalysis and Manufacture*, Springer-Verlag, Heidelberg, **1995**.
[3] B. E. Smith, *Science* **2002**, *297*, 1654–1655.
[4] a) D. V. Yandulov, R. R. Schrock, *Science* **2003**, *301*, 76–78; b) K. Arashiba, Y. Miyake, Y. Nishibayashi, *Nat. Chem.* **2011**, *3*, 120–125; c) M. Yuki, H. Tanaka, K. Sasaki, Y. Miyake, K. Yoshizawa, Y. Nishibayashi, *Nat. Commun.* **2012**, *3*, 1–6; d) M. Kitano, Y. Inoue, Y. Yamazaki, F. Hayashi, S. Kanbara, S. Matsuishi, T. Yokoyama, S. W. Kim, M. Hara, H. Hosono, *Nat. Chem.* **2012**, *4*, 934–940.
[5] a) P. L. Yue, F. Khan, L. Rizzuti, *Chem. Eng. Sci.* **1983**, *38*, 1893–1900; b) Y. Nishibayashi, M. Saito, S. Uemura, S. Takekuma, H. Takekuma, Z. Yoshida, *Nature* **2004**, *428*, 279–280; c) C. Zhong, W. B. Hu, Y. F. Cheng, *J. Mater. Chem. A* **2013**, *1*, 3216–3238.
[6] a) G. Marnellos, *Science* **1998**, *282*, 98–100; b) S.-Y. Zhang, X.-Y. Zhang, Z.-S. Zhang, Y. Kong, S.-N. Hua, *Chem. Lett.* **2003**, *32*, 440–441; c) T. Murakami, T. Nishikiori, T. Nohira, Y. Ito, *J. Am. Chem. Soc.* **2002**, *124*, 334–335; d) T. Murakami, T. Nohira, T. Goto, Y. H. Ogata, Y. Ito, *Electrochim. Acta* **2005**, *50*, 5423–5426.
[7] a) A. Fujishima, K. Honda, *Bull. Chem. Soc. Jpn.* **1971**, *44*, 1148–1150; b) A. Fujishima, K. Honda, *Nature* **1972**, *238*, 37–38.
[8] G. N. Schrauzer, T. D. Guth, *J. Am. Chem. Soc.* **1977**, *99*, 7189–7193.
[9] a) M. Grätzel, *Acc. Chem. Res.* **1981**, *14*, 376–384; b) Y. Tian, T. Tatsuma, *J. Am. Chem. Soc.* **2005**, *127*, 7632–7637.
[10] a) O. Rusina, A. Eremenko, G. Frank, H. P. Strunk, H. Kisch, *Angew. Chem.* **2001**, *113*, 4115–4117; *Angew. Chem. Int. Ed.* **2001**, *40*, 3993–3995; b) O. P. Linnik, H. Kisch, *Mendeleev Commun.* **2008**, *18*, 10–11.
[11] X. Shi, K. Ueno, N. Takabayashi, H. Misawa, *J. Phys. Chem. C* **2013**, *117*, 2494–2499.
[12] a) Y. Nishijima, K. Ueno, Y. Yokota, K. Murakoshi, H. Misawa, *J. Phys. Chem. Lett.* **2010**, *1*, 2031–2036; b) Y. Nishijima, K. Ueno, Y. Kotake, K. Murakoshi, H. Inoue, H. Misawa, *J. Phys. Chem. Lett.* **2012**, *3*, 1248–1252; c) K. Ueno, H. Misawa, *J. Photochem. Photobiol. C* **2013**, *15*, 31–52; d) K. Ueno, H. Misawa, *NPG Asia Materials* **2013**, *5*, e61.
[13] a) K. Setoura, D. Werner, S. Hashimoto, *J. Phys. Chem. C* **2012**, *116*, 15458–15466; b) H. Yamauchi, S. Ito, K. Yoshida, T. Itoh, Y. Tsuboi, N. Kitamura, H. Miyasaka, *J. Phys. Chem. C* **2013**, *117*, 8388–8396.
[14] J. G. Howalt, T. Bligaard, J. Rossmeisl, T. Vegge, *Phys. Chem. Chem. Phys.* **2013**, *15*, 7785–7795.
[15] a) F. Rosowski, A. Hornung, O. Hinrichsen, D. Herein, M. Muhler, G. Ertl, *Appl. Catal. A* **1997**, *151*, 443–460; b) S. Siporin, *J. Catal.* **2004**, *225*, 359–368.
[16] C. E. Bower, T. H. Hansen, *Can. J. Fish. Aquat. Sci.*, *37*, **1980**, 794–798.
[17] M. A. Eberhardt, J. M. Sieburth, *Mar. Chem.* **1985**, *17*, 199–212.

